



Article scientifique

Article

2022

Published version

Open Access

This is the published version of the publication, made available in accordance with the publisher's policy.

Transposon-Directed Insertion-Site Sequencing Reveals Glycolysis Gene *gpmA* as Part of the H₂O₂ Defense Mechanisms in *Escherichia coli*

Roth, Myriam; Goodall, Emily C A; Pullela, Karthik; Jaquet, Vincent; Francois, Patrice; Henderson, Ian R; Krause, Karl-Heinz

How to cite

ROTH, Myriam et al. Transposon-Directed Insertion-Site Sequencing Reveals Glycolysis Gene *gpmA* as Part of the H₂O₂ Defense Mechanisms in *Escherichia coli*. In: *Antioxidants*, 2022, vol. 11, n° 10, p. 2053. doi: [10.3390/antiox11102053](https://doi.org/10.3390/antiox11102053)

This publication URL: <https://archive-ouverte.unige.ch/unige:165177>

Publication DOI: [10.3390/antiox11102053](https://doi.org/10.3390/antiox11102053)



Article

Transposon-Directed Insertion-Site Sequencing Reveals Glycolysis Gene *gpmA* as Part of the H₂O₂ Defense Mechanisms in *Escherichia coli*

Myriam Roth ^{1,*} , Emily C. A. Goodall ², Karthik Pullela ², Vincent Jaquet ^{1,3} , Patrice François ⁴ , Ian R. Henderson ² and Karl-Heinz Krause ¹

¹ Department of Pathology and Immunology, Faculty of Medicine, University of Geneva, 1211 Geneva, Switzerland

² Institute for Molecular Bioscience, University of Queensland, St. Lucia, Brisbane, QLD 4072, Australia

³ READS Unit, Faculty of Medicine, University of Geneva, 1211 Geneva, Switzerland

⁴ Genomic Research Laboratory, Infectious Diseases Service, University Hospitals of Geneva, University Medical Center, Michel-Servet 1, 1211 Geneva, Switzerland

* Correspondence: myriam.roth@unige.ch

Abstract: Hydrogen peroxide (H₂O₂) is a common effector of defense mechanisms against pathogenic infections. However, bacterial factors involved in H₂O₂ tolerance remain unclear. Here we used transposon-directed insertion-site sequencing (TraDIS), a technique allowing the screening of the whole genome, to identify genes implicated in H₂O₂ tolerance in *Escherichia coli*. Our TraDIS analysis identified 10 mutants with fitness defect upon H₂O₂ exposure, among which previously H₂O₂-associated genes (*oxyR*, *dps*, *dksA*, *rpoS*, *hfq* and *polA*) and other genes with no known association with H₂O₂ tolerance in *E. coli* (*corA*, *rbsR*, *nhaA* and *gpmA*). This is the first description of the impact of *gpmA*, a gene involved in glycolysis, on the susceptibility of *E. coli* to H₂O₂. Indeed, confirmatory experiments showed that the deletion of *gpmA* led to a specific hypersensitivity to H₂O₂ comparable to the deletion of the major H₂O₂ scavenger gene *katG*. This hypersensitivity was not due to an alteration of catalase function and was independent of the carbon source or the presence of oxygen. Transcription of *gpmA* was upregulated under H₂O₂ exposure, highlighting its role under oxidative stress. In summary, our TraDIS approach identified *gpmA* as a member of the oxidative stress defense mechanism in *E. coli*.

Keywords: *E. coli*; H₂O₂; TraDIS; Tn-seq; phosphoglycerate mutase; *gpmA*



Citation: Roth, M.; Goodall, E.C.A.; Pullela, K.; Jaquet, V.; François, P.; Henderson, I.R.; Krause, K.-H.

Transposon-Directed Insertion-Site Sequencing Reveals Glycolysis Gene *gpmA* as Part of the H₂O₂ Defense Mechanisms in *Escherichia coli*.

Antioxidants **2022**, *11*, 2053. <https://doi.org/10.3390/antiox11102053>

Academic Editors: Danila Limauro and Emilia Pedone

Received: 30 September 2022

Accepted: 14 October 2022

Published: 18 October 2022

Publisher's Note: MDPI stays neutral with regard to jurisdictional claims in published maps and institutional affiliations.



Copyright: © 2022 by the authors. Licensee MDPI, Basel, Switzerland. This article is an open access article distributed under the terms and conditions of the Creative Commons Attribution (CC BY) license (<https://creativecommons.org/licenses/by/4.0/>).

1. Introduction

Escherichia coli is a Gram-negative facultative anaerobic bacterium. It is a frequent member of the normal human microbiota but can also be a pathogen causing food poisoning, urinary tract infection and even septic shock [1]. The burden of diarrheal infections by pathogenic strains of *E. coli* is immense; in 79 low-income countries alone, more than 200 million episodes of childhood diarrhea due to *E. coli* and *Shigella* occur each year [2]. In high-income countries, *E. coli* is the primary cause of blood stream infections, accounting for 27% of the documented bacteremia episodes [3]. The emergence of antibiotic resistance in Gram-negative bacteria is also concerning and a recent study of 203 countries identified *E. coli* as the leading pathogen for deaths associated with antimicrobial resistance in 2019 [4].

Reactive oxygen species (ROS), and more specifically hydrogen peroxide (H₂O₂), have a strong impact on bacterial pathogenesis. Millimolar H₂O₂ can be produced by certain strains of *Lactobacilli* of the human normal microbiota [5]. H₂O₂ production prevents the colonization by pathogens of the urinary tract [6]. Similarly, H₂O₂ is produced by phagocytes during the oxidative burst, a necessary step for the killing of pathogens [7]. The effect of H₂O₂ on bacteria has been partially studied, but a complete picture of how

H₂O₂ affects bacteria and the bacterial response has not been elucidated for any bacterial species. Previous studies on H₂O₂ tolerance, using DNA microarrays and RNA-seq, identified genes regulated under H₂O₂ exposure [8–10] in *E. coli*. These studies permitted a better understanding of the regulation of numerous genes and pathways affected by H₂O₂ exposure. In particular, OxyR, a specific H₂O₂-responsive transcription factor, and SoxR which senses oxidative stress and nitric oxide, have been identified as playing an important role in resistance to H₂O₂ [9,11]. OxyR senses hydrogen peroxide through the oxidation of its cysteine residues, which orchestrate a conformational change allowing it to regulate the expression of 38 genes [9,12]. The iron–sulfur cluster of SoxR is oxidized by redox cycling compounds or superoxide, leading to the activation of the transcription factor which regulates the expression of 11 genes, which includes SoxS, another transcription factor that further regulates 34 genes [9,13]. However, transcriptional analyses do not identify genes required for survival in oxidative conditions. Diverse mutagenesis techniques were used to identify the genes involved in *E. coli* survival under H₂O₂ exposure, but only a limited number of genes were identified each time [14–16].

The combination of transposon mutagenesis and high-throughput sequencing is a powerful technique that allows interrogation of the whole genome and represents a new standard for global functional genomic studies [17]. Here, we performed transposon-directed insertion-site sequencing (TraDIS) [18] to identify genes implicated in tolerance to exogenous H₂O₂ exposure. A similar approach was used on *Salmonella* Typhimurium to identify genes implicated in H₂O₂ tolerance, deepening the understanding of how the bacteria survive oxidative burst [19,20]. The results of our study highlighted the role of *gpmA*, which encodes a phosphoglycerate mutase, an enzyme of the glycolysis, under H₂O₂ exposure. This is the first study identifying *gpmA* as a factor of H₂O₂ tolerance in *E. coli*.

2. Materials and Methods

2.1. Bacterial Strains, Media and Growth Conditions

All bacterial strains and plasmid used in this study are documented in Table 1. *E. coli* strains were cultured at 37 °C in Luria–Bertani (LB) (Becton & Dickinson, Basel, Switzerland) broth or on Luria–Bertani Agar (Becton & Dickinson). H₂O₂ 35% *w/w* (Acros Organics, VWR Life Science, Nyon, Switzerland) was added at the indicated final concentration. LB was supplemented with 0.4% glucose, 0.4% glycerol, 0.4% sodium acetate, 0.4% sodium citrate, 50 mM sodium nitrate (Sigma-Aldrich, St. Louis, MI, USA, Merck and Cie, Schaffhausen, Switzerland) where indicated. Minimal medium M9 plates, constituted by M9 salts (VWR Life Science), 0.1 mM CaCl₂ (Sigma-Aldrich), 0.2 mM MgSO₄ (Sigma-Aldrich), 1.5% (*w/v*) agar (Carl Roth, Arlesheim, Switzerland), were used when indicated. Antibiotics were used when indicated at the following concentrations: ampicillin 100 µg/mL (10044, Sigma-Aldrich), kanamycin 50 µg/mL (PanReac AppliChem, VWR, Switzerland). For anaerobic assays, bacteria were grown in deoxygenated LB with the corresponding antibiotic and every step was performed under anaerobic condition (Coy Laboratory Products, Labgene scientific SA, Châtel-Saint-Denis, Switzerland). Overnight cultures and agar plates were grown overnight at 40 °C in anaerobic chamber.

Table 1. Bacterial strains and plasmid used in this study.

Name	Genotype	Source or Reference
BW25113	F ⁻ , Δ(<i>araD-araB</i>)567, Δ <i>lacZ</i> 4787(::rrnB-3), <i>rph-1</i> , Δ(<i>rhaD-rhaB</i>)568, <i>hsdR514</i>	CGSC ¹ [21]
MG1655	F ⁻ , λ ⁻ , <i>rph-1</i>	CGSC ¹
BEFB02	MG1655, Δ <i>oxyR</i> ::Cm ^r	[22]
JW3914	BW25113, Δ <i>katG</i> :: <i>kan</i>	[21]
Δ <i>katG</i>	MG1655, Δ <i>katG</i> :: <i>kan</i>	This study
JW0738	BW25113, Δ <i>gpmA</i> :: <i>kan</i>	[21]

Table 1. Cont.

Name	Genotype	Source or Reference
<i>ΔgpmA</i>	MG1655, <i>ΔgpmA::kan</i>	This study
JW4130	BW25113, <i>Δhfq::kan</i>	[21]
<i>Δhfq</i>	MG1655, <i>Δhfq::kan</i>	This study
JW0797	BW25113, <i>Δdps::kan</i>	[21]
<i>Δhfq</i>	MG1655, <i>Δdps::kan</i>	This study
JW3789	BW25113, <i>ΔcorA::kan</i>	[21]
<i>Δhfq</i>	MG1655, <i>ΔcorA::kan</i>	This study
JW5437	BW25113, <i>ΔrpoS::kan</i>	[21]
<i>ΔrpoS</i>	MG1655, <i>ΔrpoS::kan</i>	This study
JW3732	BW25113, <i>ΔrbsR::kan</i>	[21]
<i>ΔrbsR</i>	MG1655, <i>ΔrbsR::kan</i>	This study
JW0141	BW25113, <i>ΔdksA::kan</i>	[21]
<i>ΔdksA</i>	MG1655, <i>ΔdksA::kan</i>	This study
JW0018	BW25113, <i>ΔnhaA::kan</i>	[21]
<i>ΔnhaA</i>	MG1655, <i>ΔnhaA::kan</i>	This study
JW3587	BW25113, <i>ΔgpmM::kan</i>	[21]
<i>ΔgpmM</i>	MG1655, <i>ΔgpmM::kan</i>	This study
pWSK29	AmpR	[23]

¹ *E. coli* Genetic Stock Center.

The TraDIS screen was performed using a library of transposon mutants previously generated in *E. coli* strain BW25113 [18]. The *E. coli* strain MG1655 is referred in this paper as the wild-type (WT). The strain BEFB02 with *oxyR* deletion was a kind gift from B. Ezraty. Other gene deletions were obtained from the Keio collection [21] and transduced in a MG1655 background by P1 transduction.

2.2. TraDIS

The TraDIS library was thawed and diluted in 50 mL of LB broth to reach an OD₅₉₅ of 0.02 (approximately 8×10^8 CFU). H₂O₂ was added to H₂O₂-treated samples to reach a concentration of 2.5 mM whereas pure medium was added in untreated controls. The experiment was performed in duplicates. Bacteria were grown at 37 °C in aerating conditions (250 mL flask, shaking 250 rpm) until an OD₅₉₅ = 1.

Bacteria were collected and the DNA was extracted using a DNeasy Blood & Tissue Kit (Qiagen) according to the manufacturer's instructions. Samples were prepared for sequencing as described previously [18]. Briefly, genomic DNA was fragmented by ultrasonication, fragments were end-repaired using the NEBNext Ultra I kit (New England Biolabs, Notting Hill, Australia) and transposon fragments enriched by PCR using primers specific for the transposon and adapter. Samples were quantified by qPCR using the NEBNext Library Quant Kit for Illumina kit (New England Biolabs) according to the manufacturer's instructions and sequenced using an Illumina MiSeq with 150-cycle v3 cartridges.

The TraDIS data were analyzed using Bio::TraDIS pipeline [24] with the following parameters: 50 reads per gene as minimal threshold and 5% trim at each side of gene to avoid the consideration of meaningless transposon insertions that can occur within gene extremities. Sequencing reads were mapped to the *E. coli* BW25113 reference genome (accession: CP009273.1) downloaded from NCBI. Sequencing reads are available at the European Nucleotide Archive (ENA) at EMBL-EBI under accession number PRJEB56340 (<https://www.ebi.ac.uk/ena/browser/view/PRJEB56340>, accessed on 13 October 2022). Processed data are available for viewing at our online browser: <https://tradis-vault.qfab.org/>.

2.3. P1 Transduction

Strains from the Keio library were grown with 50 mg/mL kanamycin. The deletions of genes of interest from the corresponding Keio library mutant were transduced in *E. coli* MG1655 using phage P1 as previously described [25]. P1 phage was a kind donation from G. Panis (University of Geneva). The deleted mutants were verified using PCR with appropriate gene-specific primers (Supplementary Table S1).

2.4. H₂O₂ Susceptibility Assessed by Disk Diffusion Assay

To assess the susceptibility to H₂O₂ and other oxidants, we used disk diffusion assay as previously described [10]. Briefly, an overnight culture of bacteria was diluted in LB to McFarland 0.5 using a Densimat (bioMérieux, Marcy-l'Étoile, France) and LB agar plates were inoculated using a sterile cotton swab. Sterile cellulose disks (5 mm diameter) were placed on the plate and 10 µL of 1 M H₂O₂ diluted in sterile water was added to the center of the disk. Other oxidants were used at the following concentrations: methylhydroquinone (Sigma-Aldrich) MHQ 0.5 M in water; methyl viologen dichloride hydrate, also called paraquat, (Sigma-Aldrich) PQ 1 M in water; diamide (Sigma-Aldrich) DI 0.2 M in water; menadione (Sigma-Aldrich) K3 360 mM in DMSO; cumene hydroperoxide (Sigma-Aldrich) CHP 0.25 M in DMSO; sodium hypochlorite (Sigma-Aldrich) NaOCl 5%; ciprofloxacin (Sigma-Aldrich) CIP 0.5 µg/µL in water; ampicillin AMP 1 µg/µL in water.

Plates were incubated at 37 °C for 18 h and the diameter of inhibition was measured in mm. The area of inhibition was calculated as: $[\text{diameter of inhibition}/2]^2 \times 3.14$. To compare the effect of different oxidants, data were normalized as following: $[\text{area of inhibition of the interested mutant}] \times 100/[\text{area of inhibition of the WT}]$.

2.5. H₂O₂ Survival Assay

For survival assay, the susceptibility of *E. coli* to H₂O₂ was tested in liquid medium. Briefly, overnight cultures were diluted to 2×10^7 CFU/mL in 10 mL LB. 1 mL of H₂O₂ diluted in LB was added to the bacterial suspension to reach a final concentration of 2.5 mM. The corresponding control received 1 mL LB without H₂O₂. Bacteria were grown at 37 °C, 180 rpm. At indicated time points, 20 µL of each sample were serially diluted in LB by 10-fold dilutions. 10 µL of each dilution were spotted on LB agar supplemented with 100 U/mL of bovine liver catalase (Sigma-Aldrich). Plates were incubated overnight at 37 °C. Percent survival was calculated as $[\text{CFU from H}_2\text{O}_2\text{-treated sample}/\text{CFU from untreated sample}] \times 100$.

2.6. Expression Levels Assessed by qRT-PCR

Overnight cultures were diluted in 10 mL of LB to OD₅₉₅ 0.02. These fresh cultures were grown at 37 °C, 180 rpm for 2 h to reach exponential phase. Bacterial suspension was divided in 2 mL samples, and 200 µL of H₂O₂ diluted in LB was added to reach the final concentrations indicated in the figures. The same volume of LB was added in the corresponding control conditions. Samples were incubated at 37 °C for 10 min. Subsequently, 1 mL was stabilized with 2 mL RNAprotect Bacteria Reagent (Qiagen, Hombrechtikon, Switzerland). RNA was purified using RNeasy Plus Mini Kit (Qiagen) according to the manufacturer instructions with on-column DNA digestion by RNase-Free DNase Set (Qiagen).

Quantitative PCR (qRT-PCR) was performed on RNA samples as previously described [10]. Briefly, the cDNA was produced by reverse-transcribing 500 ng of total RNA using a mix of random hexamers and oligo d(T) primers and Primescript reverse transcriptase enzyme (Takara Bio, Saint Germain-en-Laye, France). The efficiency of each pair of primers was tested with four serial dilutions of cDNA. Oligonucleotides are indicated in Table 2. PCR reactions (10 µL volume) contained 1:20 diluted cDNA, $2 \times$ Power SYBR Green Master Mix (Thermo Fisher, Fisher Scientific AG, Reinach, Switzerland), and 300 nM of forward and reverse primers. PCRs were performed on a SDS 7900 HT instrument (Thermo Fisher) with the following parameters: 50 °C for 2 min, 95 °C for 10 min, and

45 cycles of 95 °C for 15 s, 60 °C for 1 min. Each reaction was performed in three replicates on 384-well plate. Raw Ct values obtained with SDS 2.2 (Thermo Fisher) were imported into Excel and normalization factors were calculated using the GeNorm method as described by Vandesompele et al. [26]. The absence of residual genomic DNA in RNA samples was verified by performing PCR reactions without RTase with the primer pair *gyrB_N*. Significance was assessed by one-way ANOVA with ad hoc Tukey's multiple comparisons test.

Table 2. Primers used in this study.

Name	Sequence	Gene Accession ID Ecocyc	Efficiency (RT-qPCR Primers)	Reference
RT-qPCR primers				
gyrB_N_qPCR_F	GTCCTGAAAGGGCTGGATG	EG10424	1.89 (89.37%)	[27]
gyrB_N_qPCR_R	CGAATACCATGTGGTG-CAGA			
gyrB_V_qPCR_F	GAAATTCTCCTCCCAGACCA	EG10424	1.83 (82.56%)	[27]
gyrB_V_qPCR_R	GCAGTTCGTTTCATCTGCTGT			
katG_qPCR_F	GGGCCGACCTGTTATCCTC	EG10511	1.92 (92.09%)	[10]
katG_qPCR_R	ATCCAGATCCGGTTCACAGA			
gpmA_qPCR_F	AGCCATGCCTGATCCAGTTC	EG11699	2.00 (100.45%)	This study
gpmA_qPCR_R	TTCACCGGTTGGTACGACG			
hfq_qPCR_F	CTACTGTTGTCCCGTCTCGC	EG10438	2.01 (101.14%)	This study
hfq_qPCR_R	TCGGTTTCTTCGCTGTCCTG			
ahpC_qPCR_F	TGCGACCTTCGTTGTTGACC	EG11384	2.00 (100.23%)	This study
ahpC_qPCR_R	CGGAGCCAGAGTTGCTTAC			
katE_qPCR_F	TCCGGAATACGAACTGGGCT	EG10509	2.08 (108.44%)	This study
katE_qPCR_R	ATTTGCCGACACGCTGAAC			
Cloning primers for <i>gpmA</i> (EG11699)				
pWSK_gpmA_KpnI_R	GGGGTACCCGACGTTTACTTCGCTTTACCCTG			This study
pWSK_EcoRI_gpmA_F	GGAATTCATCACCAGCAAACACCGAC			This study
gpmA_His11Ala_F	CTGGTTCTGGTTCGTGCGGGCGAAAGTCAG			This study
gpmA_His11Ala_R	CTGACTTTCGCCCCGACGAACCAGAACCAG			This study

2.7. H₂O₂ Degradation Measurements by Amplex Red

Overnight cultures were diluted in LB to McFarland 1.0 using a Densimat (bioMérieux) and further diluted 10 fold in fresh LB. 10 mL were grown in a Falcon 50 at 37 °C for 2 h to reach exponential phase of growth. Pellets were washed with DPBS (Gibco Thermo Fisher) and resuspended to reach OD₅₉₅ = 0.1 in DPBS. 1 mL of H₂O₂ diluted in sterile water was added to 10 mL of bacterial suspension for a final concentration of 1 mM of H₂O₂. At indicated time points, 10 µL were taken from each sample and diluted 1:200 in DPBS; 100 µL of each sample were transferred into a 96-well black plate with clear bottom (Corning). Amplex Red (Thermo Fisher) was used to detect H₂O₂ according to manufacturer's instructions. Briefly, 100 µL of Amplex Red mix was added to each well for a final concentration of 27.5 µM Amplex Red and 0.1 UI/mL horseradish peroxidase (Sigma-Aldrich). The plate was incubated for 10 min at 37 °C and the fluorescence (excitation 535 nm, detection 595 nm) was read in a Spectramax Paradigm (Molecular Devices, Wokingham, UK). A H₂O₂ calibration curve was generated by 1:2 serial dilutions of H₂O₂ in DPBS (from 0.11 mM to 1.07 × 10⁻⁴ mM) and used to calculate the H₂O₂ concentration of the samples by linear regression.

2.8. Complementation of *gpmA*

The *E. coli* MG1655 *gpmA* gene with its native promoter was amplified from genomic DNA using KOD DNA polymerase (Toyobo) and the primers in Table 2 (gene ID Ecocyc database: EG11699). The single amino acid replacement of the 11th histidine by an alanine (*gpmA* His11Ala) was obtained by overlap PCR using primers described in Table 2. The pWSK29 plasmid [23] was a kind gift from M. Roch (Geneva University). The plasmid and the PCR products were digested with the restriction enzymes *EcoRI* and *KpnI* (Thermo Fisher) and were gel-purified using QIAquick gel cleanup kit (Qiagen). T4 ligase (New England Biolabs) was used for the ligations and the ligation products (pWSK29 with either *gpmA* or *gpmA* His11Ala) were transformed in TOP10 Chemically Competent *E. coli* (C404010, Thermo Fisher). The coding region of the two cloned plasmids was verified by Sanger sequencing. Plasmids were electroporated in either WT or Δ *gpmA* strains.

The complemented Δ *gpmA* strains (pWSK29 with either *gpmA* or *gpmA* His11Ala) were compared to the WT and the Δ *gpmA* strains harboring the pWSK29 (empty) plasmid on LB agar plates containing ampicillin 100 μ g/mL.

2.9. Software

Artemis v.18.1.0 for Windows (Wellcome Sanger Institute, Cambridge, UK) was used to visualize the TraDIS data [28]. Graphpad Prism v.9.4.1 for Windows (GraphPad Software, San Diego, CA, USA) was used for data processing, graph plotting and statistical analysis. Inkscape v.1.1.1 for Windows was used for image editing (<https://inkscape.org>). Representation on metabolic map of previously acquired RNA-seq data was performed using the metabolism tool of Ecocyc [29,30]. All TraDIS data can be visualized at <http://tradis-vault.qfab.org/>.

3. Results

3.1. TraDIS Was Performed under Sublethal H₂O₂ Exposure

To determine the optimal dose of H₂O₂ to apply for the TraDIS experiment, we tested different concentrations of H₂O₂ on the *E. coli* strain BW25113, the strain used to generate the TraDIS library [18] (Figure 1A). The application of 2.5 mM H₂O₂ increased the lag phase by 70 min, whereas 5 mM or more resulted in complete absence of bacterial growth. The growth rate of bacteria during the exponential phase (between OD 0.2 and 1.6) was identical when treated with 2.5 mM compared to no treatment.

We performed the TraDIS experiment in similar conditions with 2.5 mM H₂O₂. The H₂O₂-treated condition reached OD = 1 approximately 140 min after untreated controls. We used the genome browser Artemis to observe the insertion site of the transposons (Figure 1B). To analyze the comparative fitness of each gene under both conditions, we performed fitness analysis with the Bio::TraDIS pipeline.

In TraDIS and other Tn-seq techniques, the fitness of each gene deletion is assessed by sequencing. Mutants that are less fit in a given condition will be outcompeted and therefore less abundant, which is approximately measured by insertion frequency. To ensure the relevance of our data, we scrutinized the TraDIS data for an impact on *oxyR*. The transcription factor OxyR is a well-described H₂O₂ sensor that regulates *E. coli* antioxidant response and deletion of the gene has been shown to increase sensitivity against oxidative stress [31]. As expected, the frequency of insertions was significantly reduced after exposure to H₂O₂ indicating *oxyR* mutants are less fit than the wild type in the presence of H₂O₂ (Figure 1C). Using the values derived for *oxyR* as a threshold, we identified nine genes that displayed higher fold-change values suggesting of a role for each of these genes in H₂O₂ tolerance (Table 3). Several genes were already described in the oxidative stress response.

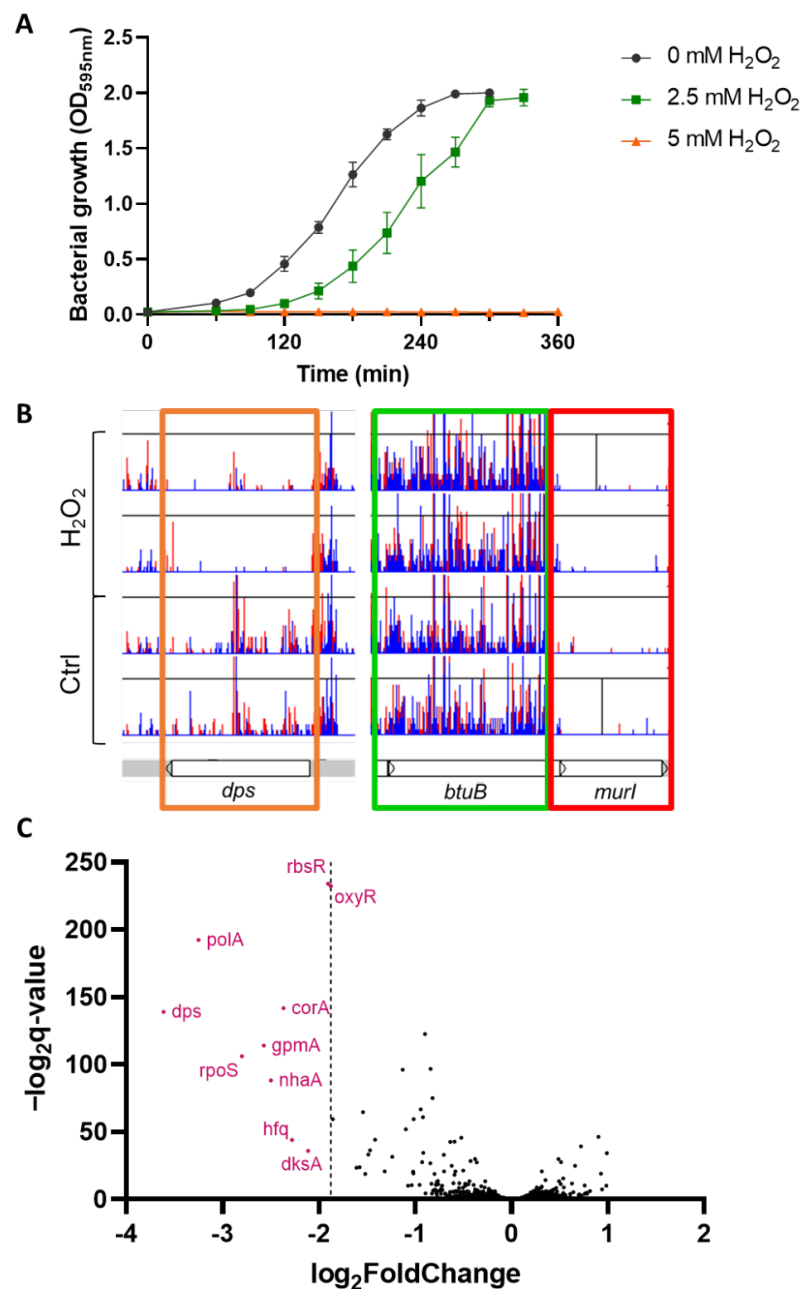


Figure 1. Transposon-directed insertion sequencing (TraDIS) screen of *E. coli* BW25113 under sublethal concentration of H_2O_2 (A) Bacterial growth of *E. coli* BW25113 over time with 2.5, 5 mM H_2O_2 and untreated control. The concentration of 2.5 mM was chosen for TraDIS experiment as it displayed a high reproducibility and a delay of approximately 70 min compared to control (mean \pm SD, $N = 3$); (B) Visualization of the TraDIS data using Artemis where each sample is represented by a histogram depicting the localization (X-axis) and the frequency (Y-axis) of transposon insertion sites (in red are antisense insertions, in blue are same sense insertions). Representative examples of essential gene (*murI* in red box), non-essential genes (*btuB*, in green box) and genes with a reduced fitness in the H_2O_2 condition (*dps* in orange box), ($N = 2$) (C) Fitness analysis of the TraDIS data, H_2O_2 -treated condition compared to control. Each dot represents a gene, X-axis represents the difference in number of insertions in the H_2O_2 condition compared to control, Y-axis represents the statistical significance. Nine genes (in pink) displayed a significant and more extreme change than the H_2O_2 -sensor gene *oxyR*.

Table 3. Genes underrepresented in the H₂O₂ condition of the TraDIS experiment. The gene function and the fold change compared to control are detailed.

Gene Name	Function	Log ₂ FC	q Value
<i>corA</i>	magnesium/nickel/cobalt transporter	−2.37	2.11 × 10 ^{−43}
<i>dksA</i>	transcriptional regulator of rRNA transcription, DnaK suppressor protein	−2.11	1.56 × 10 ^{−11}
<i>dps</i>	Fe-binding and storage protein; stress-inducible DNA-binding protein	−3.61	1.37 × 10 ^{−42}
<i>gpmA</i>	phosphoglyceromutase 1	−2.57	4.52 × 10 ^{−35}
<i>hfq</i>	global sRNA chaperone; HF-I, host factor for RNA phage Q beta replication	−2.28	5.73 × 10 ^{−14}
<i>nhaA</i>	sodium-proton antiporter	−2.50	2.71 × 10 ^{−27}
<i>oxyR</i>	oxidative and nitrosative stress transcriptional regulator	−1.88	1.17 × 10 ^{−70}
<i>polA</i>	fused DNA polymerase I 5'→3' polymerase/3'→5' exonuclease/5'→3' exonuclease	−3.25	1.29 × 10 ^{−58}
<i>rbsR</i>	transcriptional repressor of ribose metabolism	−1.90	3.27 × 10 ^{−71}
<i>rpoS</i>	RNA polymerase, sigma S (sigma 38) factor	−2.80	1.11 × 10 ^{−32}

No transposon insertion was significantly overrepresented in the H₂O₂ condition, suggesting that no gene deletion is protective against H₂O₂ in these conditions. This analysis considered only transposon insertions inside the coding regions of genes. Transposons disrupting promoters or altering the expression of genes such as polar effect were not considered by this analysis.

3.2. H₂O₂ Susceptibility of Single-Gene Deletion Identified by TraDIS

Single-deletion mutants of genes identified by the TraDIS experiments were tested against H₂O₂ to evaluate the sensitivity of each mutant. To ensure the absence of undesired mutations, cognate *E. coli* strain MG1655 mutants were created by P1 phage transduction of the relevant mutations from the Keio collection [21]. The susceptibility to H₂O₂ of the single-gene deletion mutants was assessed by disk diffusion assay. The mutant deleted for the catalase *katG*, known as the principal H₂O₂ scavenger at high concentration [32], was used as positive control. As expected, the deletion of *oxyR* led to a dramatic increase of the inhibition diameter generated by H₂O₂ (Figure 2). The deletion of *gpmA* increased the sensitivity to H₂O₂ to the same extent as the *katG* deletion. Similarly, loss of *hfq* also increased significantly the sensitivity to H₂O₂. Other genetic deletions did not significantly alter the H₂O₂ susceptibility in the disk diffusion assay.

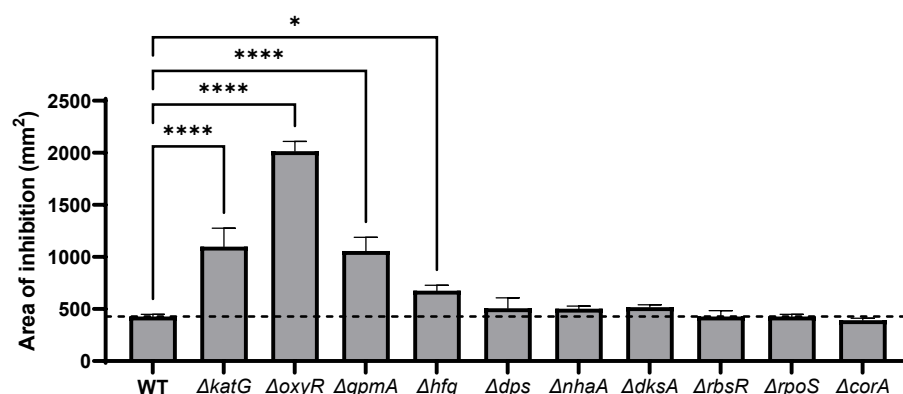


Figure 2. Sensitivity to H₂O₂ of genes identified by TraDIS. The sensitivity to 10 μL of 1 M H₂O₂ of each single-gene deletion mutant identified by the TraDIS was assessed by disk diffusion assay. The coding regions of *E. coli* MG1655 (WT) were replaced by the kanamycin cassette of the corresponding mutant originated from the Keio collection using the phage P1 to ensure the absence of undesired mutation. Data were analyzed by one-way ANOVA with Tukey test for multiple comparison and *, **** correspond to $p < 0.05$ and 0.0001 respectively (mean ± SD, $N = 3$).

3.3. $\Delta gpmA$ Mutant Was More Sensitive to H_2O_2 but Not to Other Oxidants

Single-deletion mutants were tested against other oxidants by disk diffusion assay (Figure 3). The deletion of *oxyR* and *hfq* led to an increase of the inhibition area of a wide range of oxidants (Figure 3C,E). The deletion of *gpmA* led to a hypersensitivity to H_2O_2 but not to other oxidants or antibiotics (Figure 3B,E). This pattern was highly similar to the sensitivity of the $\Delta katG$ mutant used as positive control (Figure 2E).

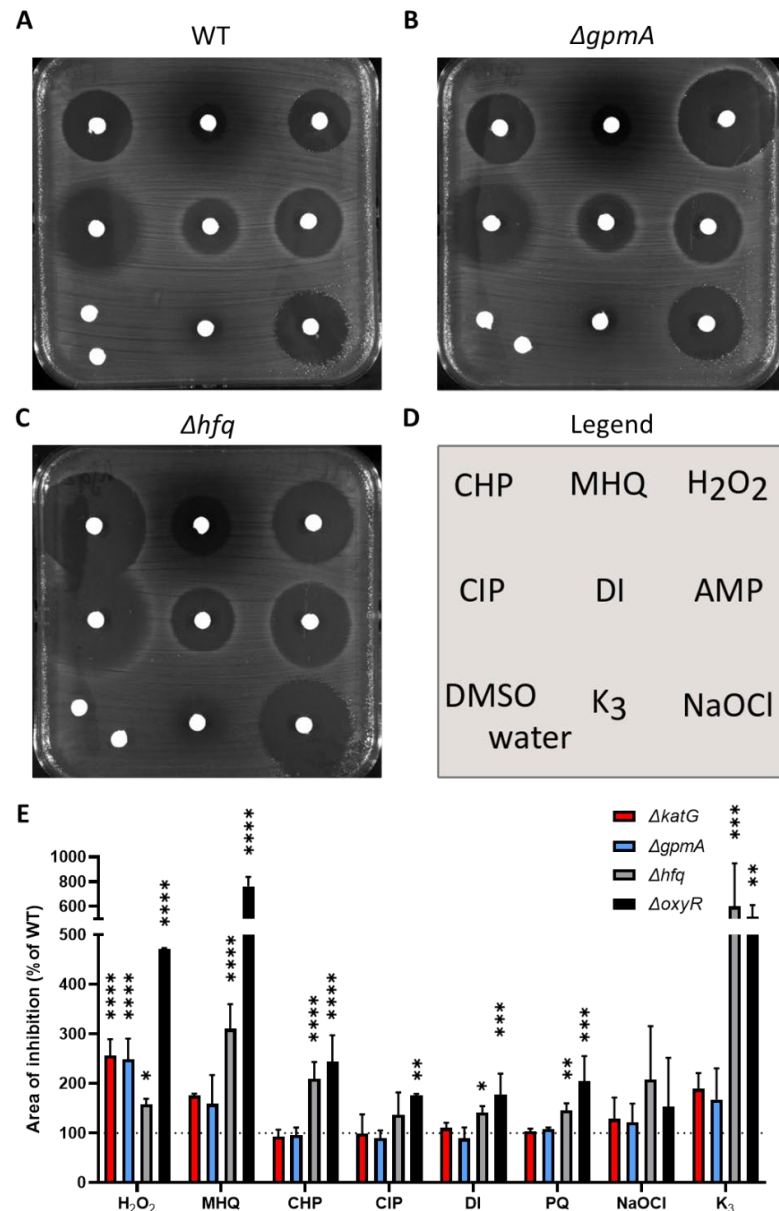


Figure 3. Sensitivity of the $\Delta oxyR$, $\Delta gpmA$ and Δhfq mutants exposed to various oxidants. (A) WT, (B) $\Delta gpmA$, (C) Δhfq . (D) Oxidants applied on each disk (CHP: cumene hydroperoxide, MHQ: methylhydroquinone, H_2O_2 : hydrogen peroxide, CIP: ciprofloxacin, DI: diamide, AMP: ampicillin, K₃: menadione, NaOCl: sodium hypochlorite, DMSO: dimethylsulfoxide). (E) Quantification of the area of inhibition normalized to WT for each oxidant. One-way ANOVA with Tukey multiple comparison was performed separately for each oxidant on the area of inhibition of the WT, $\Delta katG$ and the 9 mutants identified by TraDIS (Figure S1). The significance of the difference with the WT is represented on the normalized data by stars (mean \pm SD, $N = 3$). *, **, ***, **** correspond to $p < 0.05$, 0.01, 0.001, and 0.0001, respectively.

The deletion mutants of the other genes identified by TraDIS were also tested against these oxidants (Supplementary Materials Figure S1). The $\Delta dksA$ mutant was more sensitive to methylhydroquinone, cumene peroxide, diamide and ciprofloxacin, and the $\Delta nhaA$ mutant was slightly more sensitive to diamide and ciprofloxacin. This suggests that these mutants, despite no increased sensitivity to H_2O_2 in these conditions, were more sensitive to other oxidative stresses. Other mutants did not display significant differences compared to WT.

3.4. *gpmA* Is Upregulated by H_2O_2 Exposure

In a previous study, we performed a RNA-seq analysis of *E. coli* BW25113 after a 10 min exposure to a sublethal concentration (2.5 mM) of H_2O_2 [10]. Among the ten genes identified by TraDIS, only two genes, *dps* and *gpmA*, were significantly dysregulated by H_2O_2 (Figure 4A). In these settings, *gpmA* was upregulated over fourfold. As *gpmA* is part of the glycolysis reaction in *E. coli*, we extracted the transcriptomic data for the glycolysis and the TCA cycle (Supplementary Materials Figure S2). Other enzymes from the glycolysis (*pgi*, *pfkAB*, *fbaAB*, *pgk*) were also upregulated, suggesting an increased activity of glycolysis following exposure to H_2O_2 .

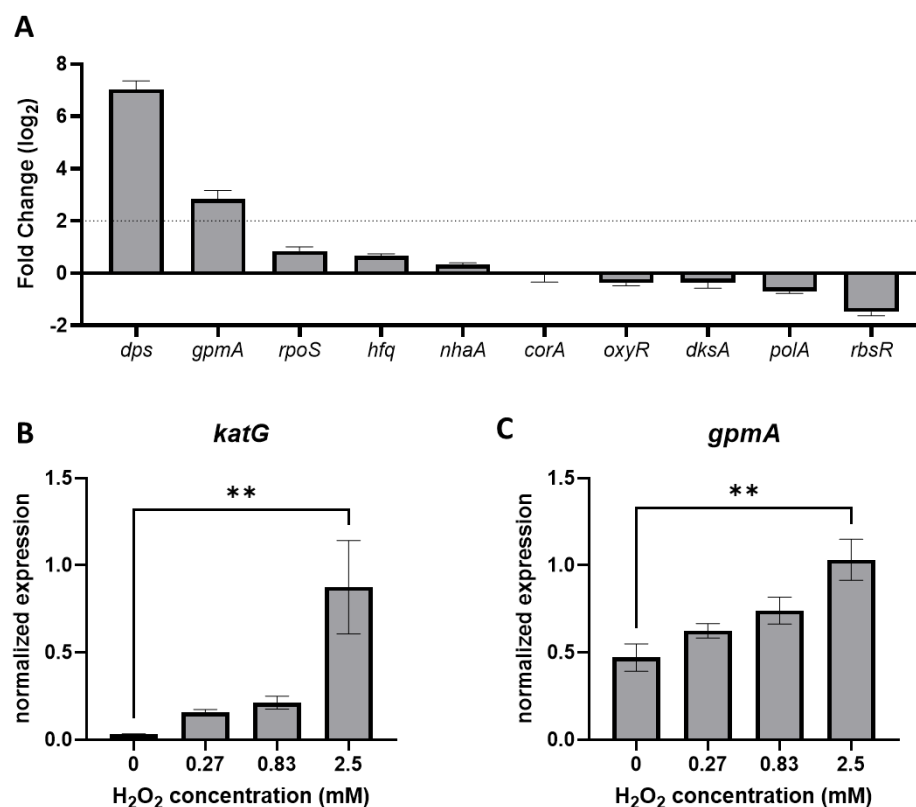


Figure 4. *gpmA* expression is upregulated following exposure to H_2O_2 . (A) Differential expression of the 10 genes identified by TraDIS 10 min after exposure to 2.5 mM H_2O_2 compared to no treatment (mean \pm SD, $N = 4$). Data originated from previously performed RNA-seq (deposited on ENA with the accession number: PRJEB51098) [10]. (B,C) Levels of expression of *katG* and *gpmA*, respectively, in the strain MG1655 under increasing concentration of H_2O_2 , assessed by qRT-PCR, ** corresponds to $p < 0.01$. (SEM \pm SD, $N = 3$).

We confirmed the impact of H_2O_2 on *gpmA* expression in the MG1655 strain used in this study by qRT-PCR. The *gpmA* RNA was upregulated following sublethal exposure of H_2O_2 in a dose-dependent manner (Figure 4C). Induction of *gpmA* expression was less impressive than the catalase *katG*, a known H_2O_2 -responsive gene (Figure 4B).

3.5. Catalase Activity Is Not Involved in the Increased Sensitivity of $\Delta gpmA$ to H_2O_2

As the $\Delta gpmA$ mutant displayed a similar sensitivity to oxidants compared to the $\Delta katG$ mutant (Figure 3E), we measured catalase expression and activity in the presence of H_2O_2 . The $\Delta gpmA$ mutant did not exhibit a growth defect compared to the WT in liquid LB (Supplementary Figure S3), so we first assessed the sensitivity of the $gpmA$ mutant to H_2O_2 in liquid LB medium by counting surviving bacteria after H_2O_2 exposure (Figure 5A). Two hours after the addition of 2.5 mM H_2O_2 , a 100-fold difference in the number of surviving bacteria in the $gpmA$ and the $oxyR$ mutant compared to the WT was observed (Figure 5B).

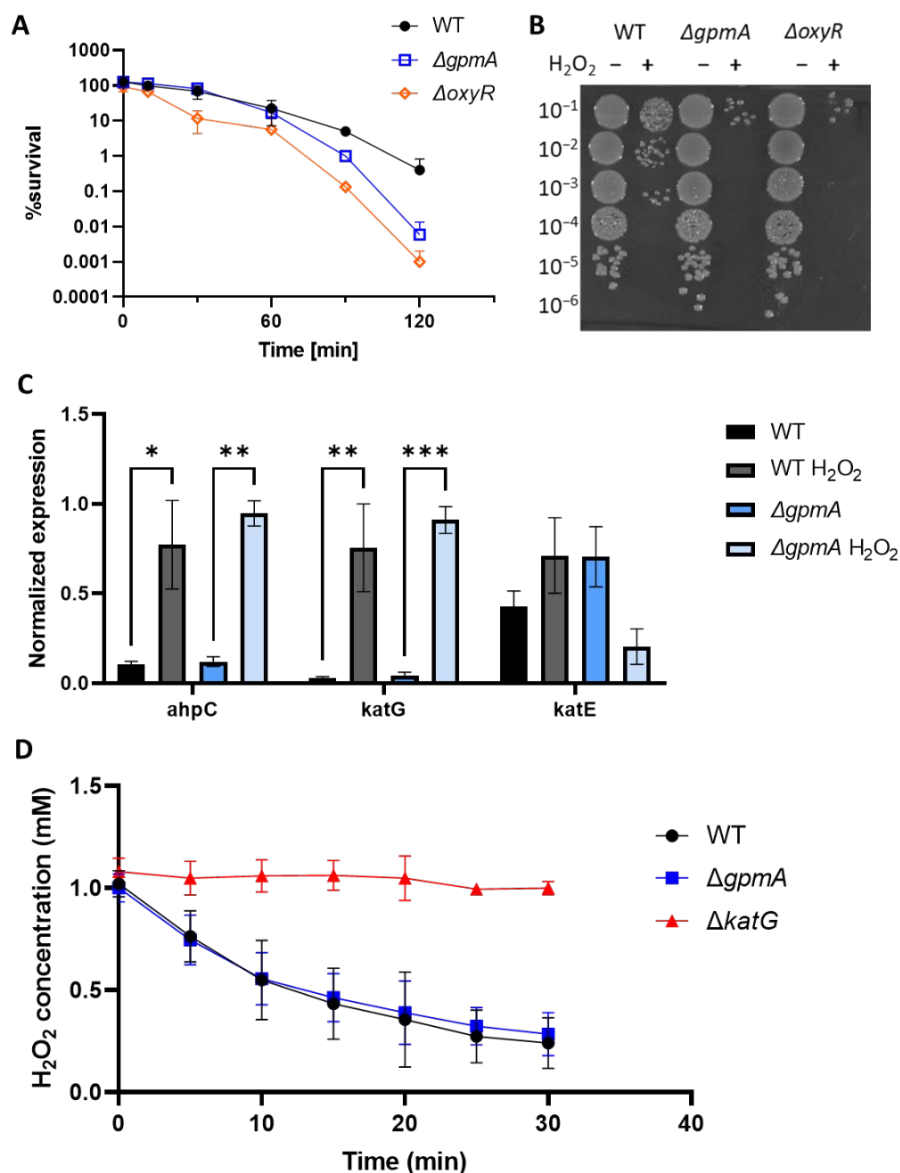


Figure 5. WT and $gpmA$ displayed no difference in catalase expression and activity. **(A)** Survival of 2×10^7 cells of WT (black), $\Delta gpmA$ (blue) and $\Delta oxyR$ (orange) over time after an exposure to 2.5 mM H_2O_2 in liquid LB (mean \pm SD, $N = 3$). **(B)** Representative image of the survival 2h after H_2O_2 treatment. Each spot represents 10 μ L at the given dilution factor. **(C)** Expression levels of *ahpC*, *katG* and *katE* in WT (black) or $\Delta gpmA$ (blue) 10 min after the addition of 2.5 mM H_2O_2 or corresponding control (mean \pm SEM, $N = 3$). Data were analyzed by Welch T-test, and *, **, *** correspond to $p < 0.05$, 0.01, 0.001, respectively. **(D)** Degradation of 1 mM H_2O_2 over time by WT (black), $\Delta gpmA$ (blue) and $\Delta katG$ (red) assessed by Amplex Red (mean \pm SD, $N = 3$).

We measured the expression levels of the three enzymes of *E. coli* that are known to degrade H₂O₂, the alkyl hydroperoxide reductase encoded by *ahpC*, the catalase/hydroperoxidase HPI encoded by *katG* and the catalase HPII encoded by *katE*. We compared the WT and the $\Delta gpmA$ strain, in presence or in absence of H₂O₂ (Figure 5C). There was no significant difference in the expression of the three genes between the WT and the $\Delta gpmA$ strain. Upregulation of *ahpC* and *katG* was observed after the addition of 2.5 mM of H₂O₂ in both strains. There was no significant difference in *katE* expression after H₂O₂ exposure, which was expected as it is not regulated by OxyR but by RpoS and upregulated during the stationary phase of bacterial growth [33].

To test if the catalase activity was affected by the deletion of *gpmA*, we measured the degradation of 1 mM of H₂O₂ of the WT and the $\Delta gpmA$ using the H₂O₂-sensitive probe Amplex Red. There was no difference in H₂O₂ degradation between the WT and the $\Delta gpmA$ strains. The $\Delta katG$ strain, which is defective for the main H₂O₂ scavenger at high concentration, was unable to degrade H₂O₂. Altogether, this suggests that the higher sensitivity of the $\Delta gpmA$ to H₂O₂ is independent of catalase activity.

3.6. Other Carbon Sources Cannot Compensate the H₂O₂ Hypersensitivity of $\Delta gpmA$ Mutant

In LB medium, amino acids are the main source of carbon and there is virtually no glucose [34]. We wondered if the supplementation with metabolites entering the central metabolism at different levels could affect the H₂O₂ sensitivity of the $\Delta gpmA$ mutant. The addition of alternative carbon source did not significantly modify the H₂O₂ susceptibility of the WT or the $\Delta gpmA$ mutant (Figure 6A). We also tested H₂O₂ sensitivity in M9 minimal media with these metabolites as the only carbon source. There was no difference in the sensitivity of the WT in M9 + glucose compared to LB + glucose. The WT strain was slightly more sensitive in M9 + acetate compared to M9 + glucose. The $\Delta gpmA$ strain displayed a higher sensitivity in the M9 conditions compared to LB conditions. M9 plates with citrate as the sole source of carbon led to limited growth even after 48 h and were therefore not measurable. Addition of 0.5% pyruvate led to a complete disappearance of the zone of inhibition (data not shown) probably because pyruvate reacts with H₂O₂ to produce CO₂, acetate and water [35].

In *Salmonella* Typhimurium, the $\Delta gpmA$ mutant was more susceptible to H₂O₂ than the WT in aerobic conditions, but not in anaerobic conditions, and the addition of the electron acceptor nitrate restored the hypersusceptibility of $\Delta gpmA$ [20]. We tested the H₂O₂ susceptibility of *E. coli* WT and $\Delta gpmA$ in anaerobic conditions. Interestingly, it appeared that the WT was slightly more sensitive to H₂O₂ in anaerobic conditions than in aerobic conditions suggesting that the exposure to oxygen protect in part against H₂O₂ damage. However, the $\Delta gpmA$ mutant did not display any difference in H₂O₂ sensitivity between anaerobic and aerobic conditions and the difference between the $\Delta gpmA$ mutant and the WT was maintained in anaerobic conditions. As *E. coli* is also able to use other electron acceptors than oxygen for respiration, we tested the addition of sodium nitrate in anaerobic conditions, but this did not change the area of inhibition induced by H₂O₂ compared to the anaerobic condition without nitrate (data not shown).

Altogether, we explored a potential impact of factors affecting glycolysis following H₂O₂ exposure, but we did not observe significant changes in conditions of low oxygen or using different carbon sources.

3.7. The Function of *gpmA* Is Necessary for H₂O₂ Tolerance

The $\Delta gpmA$ was complemented by native *gpmA* gene including its natural promoter using the low copy plasmid pWSK29. The complemented strain displayed similar H₂O₂ susceptibility than the WT strain (Figure 7A). A mutation previously described as to be necessary for the function of *gpmA*, namely the substitution of the histidine 11 residue by an alanine [36], resulted in restauration of the hypersensitivity to H₂O₂. These data suggest that the function of *gpmA* is necessary to reach the WT levels of tolerance against H₂O₂.

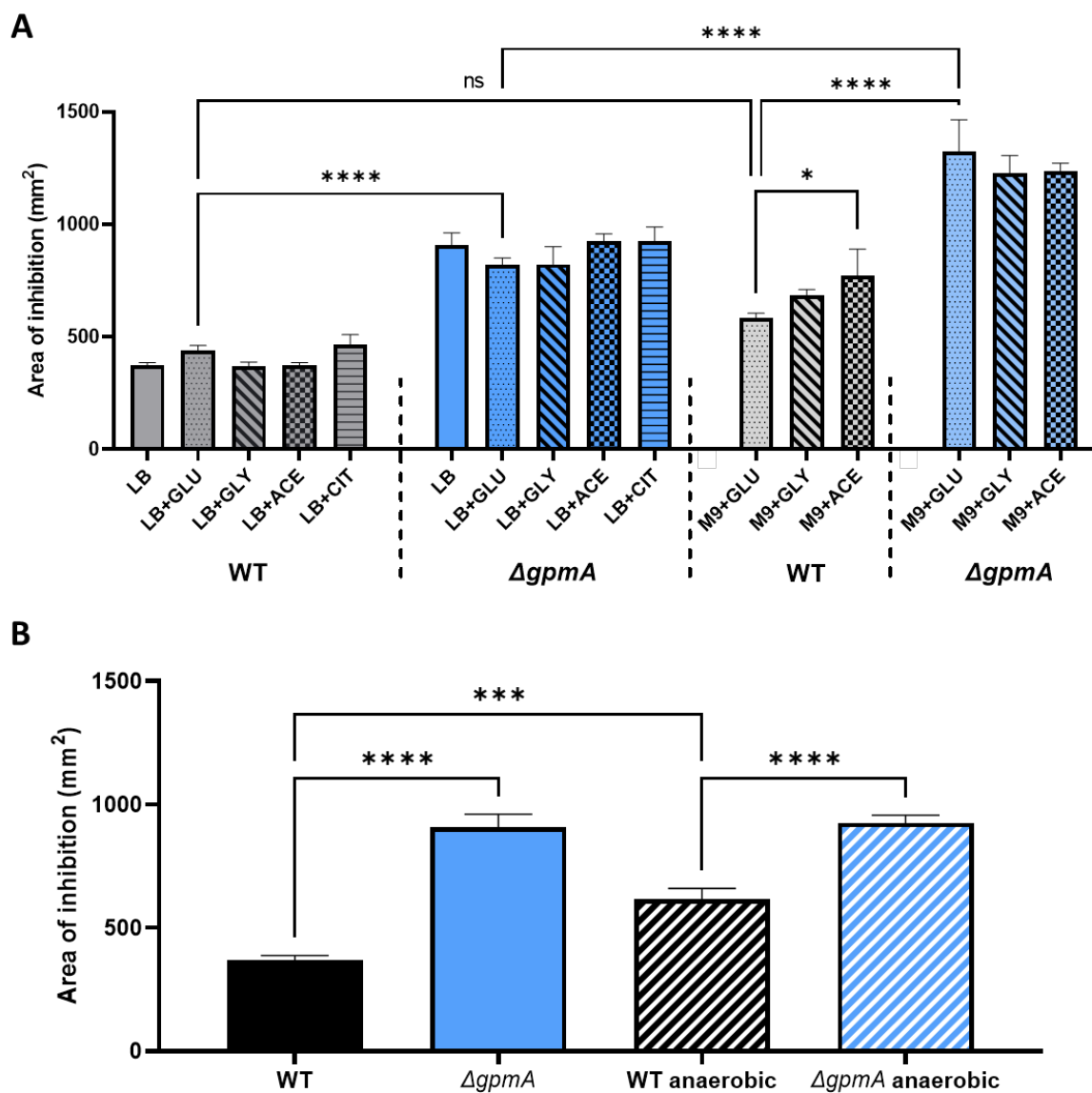


Figure 6. The difference in H₂O₂ tolerance between WT and $\Delta gpmA$ mutant is not affected by the addition of other carbon sources or the absence of oxygen. (A) Area of inhibition assessed by disk diffusion assay of WT and $\Delta gpmA$ strain on LB and M9 minimal medium complemented with diverse carbon source. GLU: glucose, GLY: glycerol, ACE: acetate, CIT: citrate (mean \pm SD, $N = 3$). (B) Area of inhibition of the WT and $\Delta gpmA$ strain under aerobic and anaerobic conditions (mean \pm SD, $N = 3$). Data in (A,B) were analyzed by one-way ANOVA with Tukey test for multiple comparison, and *, ***, **** correspond to $p < 0.05$, 0.001, 0.0001 respectively.

E. coli possess a secondphosphoglycerate mutase encoded by *gpmM*, which presents no sequence similarity with *gpmA* [37]. Contrary to *gpmA*, the expression level of *gpmM* was slightly downregulated after the addition of H₂O₂ in a previous RNA-seq dataset (Figure 7B). This suggests that following exposure to H₂O₂, *gpmA* represents the principal form of phosphoglycerate mutase. We tested the $\Delta gpmM$ mutant for H₂O₂ sensitivity. Contrary to *gpmA*, the deletion of *gpmM* did not increase the sensitivity to H₂O₂ (Figure 7C), suggesting a possible alternative function of *gpmA* in conditions of H₂O₂ exposure.

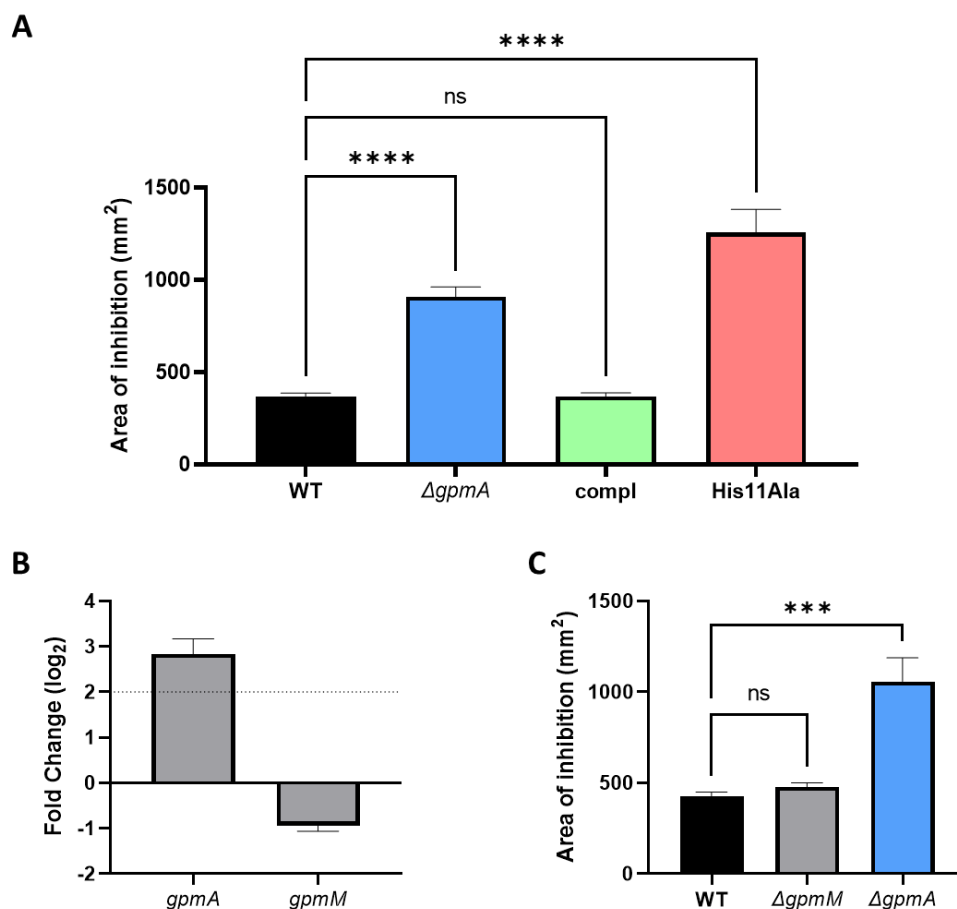


Figure 7. The function of *gpmA*, but not *gpmM*, is necessary to reach WT level of H₂O₂ tolerance. (A) Sensitivity to H₂O₂ assessed by disk diffusion assay for the WT with the empty plasmid, the $\Delta gpmA$ mutant with the empty plasmid, the $\Delta gpmA$ mutant with the plasmid encoding the native sequence of *gpmA* (compl) and the $\Delta gpmA$ mutant complemented with the plasmid encoding *gpmA* with the replacement of the histidine 11 by an alanine (His11Ala). All tests were performed in LB + ampicillin. Data were analyzed by one-way ANOVA with Tukey test for multiple comparison and **** correspond to $p < 0.0001$ (mean \pm SD, $N = 3$). (B) Differential expression of *gpmA* and *gpmM* 10 min after exposition to 2.5 mM H₂O₂ compared to no treatment (mean \pm SD, $N = 4$). Data from previously performed RNA-seq (deposited on ENA with the accession number: PRJEB51098) [10]. (C) Sensitivity to H₂O₂ assessed by disk diffusion assay of WT, $\Delta gpmA$ and $\Delta gpmM$ mutants. Data were analyzed by Welch *t*-test and *** correspond to $p < 0.001$ (mean \pm SD, $N = 3$).

4. Discussion

The production of H₂O₂ by phagocytes from the human immune system and by *Lactobacilli* species of the normal microbiota are essential for the prevention of colonization from various opportunistic pathogens. Although H₂O₂ effects on bacteria have been studied for years, the mechanisms by which H₂O₂ exerts its antimicrobial activity is still incompletely understood [14,16].

Our TraDIS analysis identified 10 mutants with fitness defect upon H₂O₂ exposure, implicating a role for these genes under H₂O₂-induced oxidative stress. Only three of the ten genes, *oxyR*, *gpmA* and *hfq*, showed a significantly higher susceptibility to H₂O₂ when knocked-out. This could be due to the differences in the settings between the TraDIS experiment and the disk diffusion assay. For example, the DNA-binding protein encoded by *dps* protects DNA from H₂O₂ damage through iron sequestration and this defense is more important in stationary phase of growth [38]. However stationary phase cultures of each knockout was treated with H₂O₂ in liquid medium, their respective growth was not different compared to the WT, except for the $\Delta oxyR$ strain (data not shown). The majority of

genes we identified by TraDIS (*oxyR*, *dps*, *rpoS*, *dksA*, *hfq*, *polA*) have already been reported to respond to oxidative stress in *E. coli*. The transcription factor OxyR is a well described sensor of H₂O₂, which regulates an extensive and coordinated antioxidant transcriptional response [9,39]. The RNA polymerase subunit RpoS regulates the general stress response and was previously described to be activated by oxidative stress [40], and the deletion of this gene increases sensitivity to H₂O₂ [41]. The RNA polymerase accessory protein DksA senses oxidative stress through its cysteine residues and participates to the transcriptional response against oxidative stress [42]. *Hfq*, a RNA-binding protein that affects many cellular processes influences both the small RNA OxyS and the translation of *rpoS* described above in *E. coli* [43,44]. The DNA polymerase I encoded by *polA* is implicated in DNA repair and non-functional PolA increases H₂O₂-sensitivity [45,46]. The *polA*, *rbsR*, *dps*, *oxyR*, *corA*, *rpoS* genes were also identified in a similar experiment performed previously on *Salmonella enterica* serovar Typhimurium under sublethal H₂O₂ exposure [19]. The *dksA* and *nhaA* mutants, despite showing no increase in sensitivity to H₂O₂, were slightly more sensitive to other oxidants than WT using disk diffusion assay. Other validation experiments, such as competition assay with WT under H₂O₂ stress, might better reflect the TraDIS experimental conditions.

On the other hand, several genes previously identified in the literature as necessary for H₂O₂ tolerance were not identified by this TraDIS experiment. For example, *xthA*, whose deletion mutant is more sensitive to H₂O₂ [47], displayed a decreased fitness in H₂O₂ condition but did not reach the threshold of significance. An explanation could lie in the fact that unlike antibiotics, H₂O₂ is rapidly degraded by bacteria. The duration of the exposure to H₂O₂ performed for the TraDIS may have been insufficient to identify all genes implicated in H₂O₂ tolerance. Secondly, the stress was applied against pooled mutants in liquid where other mutants could provide cross-protection for susceptible mutants. For example, the catalase KatG, which is known to protect against H₂O₂, was not identified by TraDIS, probably because of this phenomenon. This was also the case in a previous study that used Tn-seq with H₂O₂ in *Salmonella* Typhimurium, where none of the catalase genes were identified [19]. Thus, our TraDIS data only identified those mutants that showed fitness defects despite cross-protection and inherent H₂O₂ degradation.

The TraDIS experiment also identified genes that, to our knowledge, were not previously associated with *E. coli* H₂O₂ sensitivity. The magnesium ion transporter encoded by *corA* had been shown to be more sensitive to lactoperoxidase–thiocyanate stress but not to H₂O₂ [48]. *rbsR* controls the transcription of the operon involved in ribose catabolism and transport and the salvage pathway of purine nucleotide synthesis [49]. *corA* and *rbsR* were also identified in a similar Tn-seq experiment using H₂O₂ on *Salmonella enterica* serovar Typhimurium [19]. The Na⁺:H⁺ antiporter *nhaA* is implicated in other stress responses against sodium ion, pH homeostasis and in maintaining antibiotic tolerance under starvation [50]. The glycolysis enzyme *gpmA* has been previously identified by a Tn-seq experiment following H₂O₂ exposure in the Gram-negative bacteria *Salmonella enterica* serovar Typhimurium [20].

When tested with diverse oxidants that damage bacteria through different modes of action, Δ *gpmA* was specifically more sensitive to H₂O₂, like the Δ *katG* strain. However, it was not through a differential expression of H₂O₂-scavenging genes or a decreased catalase activity of the strain, suggesting a different mode of action. Moreover, the upregulation of *gpmA* by sublethal exposure of H₂O₂ suggests the importance of *gpmA* in H₂O₂ tolerance. Under oxidative stress, some enzymes of the central metabolism have been shown to be upregulated. The glucose-6-phosphate isomerase encoded by *pgi* have been shown to be regulated by the oxidative stress sensitive regulators SoxRS [51]. Similarly, in the TCA cycle, the aconitase *acnA* and the fumarase *fumC* are regulated by SoxRS and are upregulated under H₂O₂ exposure [52,53]. The hypersensitivity to H₂O₂ of Δ *gpmA* mutant could be complemented with the low-copy plasmid pWSK29 expressing the WT *gpmA* gene under its native promoter but not if the histidine 11 was mutated to an alanine. This strongly suggests that the function of *gpmA* affects *E. coli* tolerance to H₂O₂.

Surprisingly, addition of other metabolites or the absence of oxygen did not abolish the difference in H₂O₂ sensitivity between the WT and the $\Delta gpmA$ mutant. These data contrast with previous work on *Salmonella enterica* serovar Typhimurium, where other metabolites entering metabolism downstream of *gpmA* reaction (for a scheme of glycolysis, see Supplementary Figure S2) could complement the increased sensitivity of a $\Delta gpmA$ mutant and where anoxic environment abolished the difference of H₂O₂ susceptibility between WT and $\Delta gpmA$ mutant [20]. In the same study, metabolomics approach showed that H₂O₂ exposure led to an increase of glycolysis and fermentation that was important in *Salmonella* H₂O₂ tolerance. This contrasts with previous metabolomics analysis on *E. coli* after H₂O₂ treatment which reported a decrease of metabolites related to glycolysis and TCA cycle, changes that were common to other stress conditions such as heat shock and cold stress [54]. Altogether, this suggests a different metabolic adaptation to H₂O₂ stress between *E. coli* and *Salmonella* and a difference of *gpmA* function. More research is needed to better understand the mechanisms of *gpmA* effects in H₂O₂ tolerance in *E. coli* and in other organisms.

Contrary to vertebrates that only possess one phosphoglycerate mutase, some eubacteria, among which relevant pathogens including *E. coli*, encode two enzymes that display no sequence similarity [55]. The 2,3-bisphosphoglycerate-dependent phosphoglycerate mutase (or dPGM), encoded by *gpmA* is common to bacteria and vertebrates, whereas 2,3-bisphosphoglycerate-independent phosphoglycerate mutase (or iPGM) encoded by *gpmM* is shared by bacteria and higher plants. As the double deletion of *gpmA* and *gpmM* have been suspected non-viable in *E. coli*, the glycolysis function is assumed by *gpmM* in the *gpmA*-deleted strain and vice versa [56]. The deletion of *E. coli gpmM* did not affect H₂O₂ sensitivity, suggesting that only *gpmA* function has a role under H₂O₂ exposure. This led to the hypothesis that *gpmM* could be damaged by H₂O₂ and its function is replaced by *gpmA* under H₂O₂ exposure. This happens for other enzymes of the TCA cycle, the aconitase and the fumarase, where oxidative-resistant isoforms (*acnA*, *fumC*) replace oxidative-sensitive isoforms (*acnB*, *fumA*, *fumB*), after H₂O₂ exposure [52,53]. Cysteine residues can be more prone to oxidation by H₂O₂ than other amino acids [57]. GpmM possesses two cysteine residues, which can result in H₂O₂-induced damage from oxidation of these residues. As GpmA does not possess cysteine residues, it could be more resistant to H₂O₂ than GpmM. The cysteine residues of GpmM are not implicated in active sites described in current models (Ecocyc, Uniprot). While Cys397 seems buried and is not conserved in Gram-positive bacteria, Cys424 seems to be more accessible on the protein models and is present in both Gram-negative (*P. aeruginosa*, *Salmonella enterica*, *K. pneumoniae*) and Gram-positive bacteria (*S. aureus*, *B. subtilis*). Additional studies are needed to evaluate their potential implication in oxidative stress susceptibility.

5. Conclusions

This work was aimed at expanding the knowledge of which genes are implicated in H₂O₂ tolerance. The main finding of this study was that a functional *gpmA* gene is required for tolerance to H₂O₂. This is the first time that *gpmA* was highlighted as an important contributor to the *E. coli* tolerance to H₂O₂, and it links defense against oxidative stress to central metabolism.

Supplementary Materials: The following are available online at <https://www.mdpi.com/article/10.3390/antiox11102053/s1>, Table S1: Primers used to validate the gene replacement by the kanamycin cassette from the Keio collection, Figure S1: Sensitivity of the deletion mutants of the TraDIS exposed to various oxidants, Figure S2: Schematic diagram of H₂O₂-induced transcriptional changes of glycolysis and TCA cycle, Figure S3: The deletion of *gpmA* did not affect bacterial growth.

Author Contributions: Conceptualization, M.R., V.J., K.-H.K. and P.F.; methodology, E.C.A.G., K.P. and M.R.; software, E.C.A.G. and K.P.; validation, K.P.; formal analysis, E.C.A.G. and M.R.; investigation, M.R., E.C.A.G. and K.P.; resources, E.C.A.G., K.P. and I.R.H.; data curation, E.C.A.G., K.P. and M.R.; writing—original draft preparation, M.R. and V.J.; writing—review and editing, P.F.; visualization, M.R.; supervision, K.-H.K., I.R.H. and P.F.; project administration, V.J., K.-H.K., I.R.H. and P.F.; funding acquisition, K.-H.K. All authors have read and agreed to the published version of the manuscript.

Funding: This study was granted by Swiss National Science Foundation to Karl-Heinz Krause (Funding number 31003A-179478). The TraDIS work was supported by University of Queensland funding to Ian Henderson.

Institutional Review Board Statement: Not applicable.

Informed Consent Statement: Not applicable.

Data Availability Statement: The data for this study have been deposited in the European Nucleotide Archive (ENA) at EMBL-EBI under accession number PRJEB56340 (<https://www.ebi.ac.uk/ena/browser/view/PRJEB56340>). Processed data are available for viewing at our online browser: <https://tradis-vault.qfab.org/>.

Acknowledgments: The authors gratefully acknowledge Benjamin Ezraty for the donation of the MG1655 $\Delta oxyR::Cm^R$ strain; Mélanie Roch for the donation of the pWSK29 plasmid; Gaël Panis for the donation of the P1 phage; Roberto Sierra, Mélanie Roch, Gaël Panis, Clement David, Aleksander Czauderna, Simone Becattini and the collaborators of the genomics platform iGE3 of the faculty of Medicine of the University of Geneva: Didier Chollet and Mylène Docquier for technical support.

Conflicts of Interest: The authors declare no conflict of interest.

References

1. Dunne, K.A.; Chaudhuri, R.R.; Rossiter, A.E.; Beriotto, I.; Browning, D.F.; Squire, D.; Cunningham, A.F.; Cole, J.A.; Loman, N.; Henderson, I.R. Sequencing a Piece of History: Complete Genome Sequence of the Original Escherichia Coli Strain. *Microb. Genom.* **2017**, *3*, mgen000106. [[CrossRef](#)]
2. Anderson, J.D.; Bagamian, K.H.; Muhib, F.; Amaya, M.P.; Laytner, L.A.; Wierzbza, T.; Rheingans, R. Burden of Enterotoxigenic Escherichia Coli and Shigella Non-Fatal Diarrhoeal Infections in 79 Low-Income and Lower Middle-Income Countries: A Modelling Analysis. *Lancet Glob. Health* **2019**, *7*, e321–e330. [[CrossRef](#)]
3. Bonten, M.; Johnson, J.R.; van den Biggelaar, A.H.J.; Georgalis, L.; Geurtsen, J.; de Palacios, P.I.; Gravenstein, S.; Verstraeten, T.; Hermans, P.; Poolman, J.T. Epidemiology of Escherichia Coli Bacteremia: A Systematic Literature Review. *Clin. Infect. Dis.* **2021**, *72*, 1211–1219. [[CrossRef](#)]
4. Murray, C.J.; Ikuta, K.S.; Sharara, F.; Swetschinski, L.; Aguilar, G.R.; Gray, A.; Han, C.; Bisignano, C.; Rao, P.; Wool, E.; et al. Global Burden of Bacterial Antimicrobial Resistance in 2019: A Systematic Analysis. *Lancet* **2022**, *399*, 629–655. [[CrossRef](#)]
5. Pridmore, R.D.; Pittet, A.-C.; Praplan, F.; Cavadini, C. Hydrogen Peroxide Production by Lactobacillus Johnsonii NCC 533 and Its Role in Anti-Salmonella Activity. *FEMS Microbiol. Lett.* **2008**, *283*, 210–215. [[CrossRef](#)]
6. Gupta, K.; Stapleton, A.E.; Hooton, T.M.; Roberts, P.L.; Fennell, C.L.; Stamm, W.E. Inverse Association of H₂O₂-Producing Lactobacilli and Vaginal Escherichia Coli Colonization in Women with Recurrent Urinary Tract Infections. *J. Infect. Dis.* **1998**, *178*, 446–450. [[CrossRef](#)]
7. Winterbourn, C.C.; Kettle, A.J. Redox Reactions and Microbial Killing in the Neutrophil Phagosome. *Antioxid. Redox Signal.* **2013**, *18*, 642–660. [[CrossRef](#)]
8. Zheng, M.; Wang, X.; Templeton, L.J.; Smulski, D.R.; LaRossa, R.A.; Storz, G. DNA Microarray-Mediated Transcriptional Profiling of the Escherichia Coli Response to Hydrogen Peroxide. *J. Bacteriol.* **2001**, *183*, 4562–4570. [[CrossRef](#)]
9. Seo, S.W.; Kim, D.; Szubin, R.; Palsson, B.O. Genome-Wide Reconstruction of OxyR and SoxRS Transcriptional Regulatory Networks under Oxidative Stress in Escherichia Coli K-12 MG1655. *Cell Rep.* **2015**, *12*, 1289–1299. [[CrossRef](#)]
10. Roth, M.; Jaquet, V.; Lemeille, S.; Bonetti, E.-J.; Cambet, Y.; François, P.; Krause, K.-H. Transcriptomic Analysis of E. Coli after Exposure to a Sublethal Concentration of Hydrogen Peroxide Revealed a Coordinated Up-Regulation of the Cysteine Biosynthesis Pathway. *Antioxidants* **2022**, *11*, 655. [[CrossRef](#)]
11. Kobayashi, K.; Fujikawa, M.; Kozawa, T. Oxidative Stress Sensing by the Iron–Sulfur Cluster in the Transcription Factor, SoxR. *J. Inorg. Biochem.* **2014**, *133*, 87–91. [[CrossRef](#)]
12. Choi, H.-J.; Kim, S.-J.; Mukhopadhyay, P.; Cho, S.; Woo, J.-R.; Storz, G.; Ryu, S.-E. Structural Basis of the Redox Switch in the OxyR Transcription Factor. *Cell* **2001**, *105*, 103–113. [[CrossRef](#)]
13. Imlay, J.A. Transcription Factors That Defend Bacteria against Reactive Oxygen Species. *Annu. Rev. Microbiol.* **2015**, *69*, 93–108. [[CrossRef](#)]

14. Farr, S.B.; D'Ari, R.; Touati, D. Oxygen-Dependent Mutagenesis in Escherichia Coli Lacking Superoxide Dismutase. *Proc. Natl. Acad. Sci. USA* **1986**, *83*, 8268–8272. [[CrossRef](#)]
15. Mukhopadhyay, S.; Schellhorn, H.E. Identification and Characterization of Hydrogen Peroxide-Sensitive Mutants of Escherichia Coli: Genes That Require OxyR for Expression. *J. Bacteriol.* **1997**, *179*, 330–338. [[CrossRef](#)]
16. Rodríguez-Rojas, A.; Kim, J.J.; Johnston, P.R.; Makarova, O.; Eravci, M.; Weise, C.; Hengge, R.; Rolff, J. Non-Lethal Exposure to H₂O₂ Boosts Bacterial Survival and Evolvability against Oxidative Stress. *PLoS Genet.* **2020**, *16*, e1008649. [[CrossRef](#)]
17. Chao, M.C.; Abel, S.; Davis, B.M.; Waldor, M.K. The Design and Analysis of Transposon-Insertion Sequencing Experiments. *Nat. Rev. Microbiol.* **2016**, *14*, 119–128. [[CrossRef](#)]
18. Goodall, E.C.A.; Robinson, A.; Johnston, I.G.; Jabbari, S.; Turner, K.A.; Cunningham, A.F.; Lund, P.A.; Cole, J.A.; Henderson, I.R. The Essential Genome of Escherichia Coli K-12. *mBio* **2018**, *9*, e02096-17. [[CrossRef](#)]
19. Karash, S.; Liyanage, R.; Qassab, A.; Lay, J.O.; Kwon, Y.M. A Comprehensive Assessment of the Genetic Determinants in Salmonella Typhimurium for Resistance to Hydrogen Peroxide Using Proteogenomics. *Sci. Rep.* **2017**, *7*, 17073. [[CrossRef](#)]
20. Chakraborty, S.; Liu, L.; Fitzsimmons, L.; Porwollik, S.; Kim, J.-S.; Desai, P.; McClelland, M.; Vazquez-Torres, A. Glycolytic Reprograming in Salmonella Counters NOX2-Mediated Dissipation of ΔpH. *Nat. Commun.* **2020**, *11*, 1783. [[CrossRef](#)]
21. Baba, T.; Ara, T.; Hasegawa, M.; Takai, Y.; Okumura, Y.; Baba, M.; Datsenko, K.A.; Tomita, M.; Wanner, B.L.; Mori, H. Construction of Escherichia Coli K-12 in-Frame, Single-Gene Knockout Mutants: The Keio Collection. *Mol. Syst. Biol.* **2006**, *2*, 2006.0008. [[CrossRef](#)]
22. Ezraty, B.; Vergnes, A.; Banzhaf, M.; Duverger, Y.; Huguenot, A.; Brochado, A.R.; Su, S.-Y.; Espinosa, L.; Loiseau, L.; Py, B.; et al. Fe-S Cluster Biosynthesis Controls Uptake of Aminoglycosides in a ROS-Less Death Pathway. *Science* **2013**, *340*, 1583–1587. [[CrossRef](#)]
23. Wang, R.F.; Kushner, S.R. Construction of Versatile Low-Copy-Number Vectors for Cloning, Sequencing and Gene Expression in Escherichia Coli. *Gene* **1991**, *100*, 195–199. [[CrossRef](#)]
24. Barquist, L.; Mayho, M.; Cummins, C.; Cain, A.K.; Boinett, C.J.; Page, A.J.; Langridge, G.C.; Quail, M.A.; Keane, J.A.; Parkhill, J. The TraDIS Toolkit: Sequencing and Analysis for Dense Transposon Mutant Libraries. *Bioinformatics* **2016**, *32*, 1109–1111. [[CrossRef](#)]
25. Thomason, L.C.; Costantino, N.; Court, D.L.E. Coli Genome Manipulation by P1 Transduction. *Curr. Protoc. Mol. Biol.* **2007**, *1*, 1.17.1–1.17.8. [[CrossRef](#)]
26. Vandesompele, J.; De Preter, K.; Pattyn, F.; Poppe, B.; Van Roy, N.; De Paepe, A.; Speleman, F. Accurate Normalization of Real-Time Quantitative RT-PCR Data by Geometric Averaging of Multiple Internal Control Genes. *Genome Biol.* **2002**, *3*, research0034.1. [[CrossRef](#)]
27. Rocha, D.J.P.G.; Castro, T.L.P.; Aguiar, E.R.G.R.; Pacheco, L.G.C. Gene Expression Analysis in Bacteria by RT-QPCR. In *Quantitative Real-Time PCR: Methods and Protocols*; Biassoni, R., Raso, A., Eds.; Methods in Molecular Biology; Springer: New York, NY, USA, 2020; pp. 119–137, ISBN 978-1-4939-9833-3.
28. Carver, T.; Harris, S.R.; Berriman, M.; Parkhill, J.; McQuillan, J.A. Artemis: An Integrated Platform for Visualization and Analysis of High-Throughput Sequence-Based Experimental Data. *Bioinformatics* **2012**, *28*, 464–469. [[CrossRef](#)]
29. Keseler, I.M.; Collado-Vides, J.; Santos-Zavaleta, A.; Peralta-Gil, M.; Gama-Castro, S.; Muñoz-Rascado, L.; Bonavides-Martinez, C.; Paley, S.; Krummenacker, M.; Altman, T.; et al. EcoCyc: A Comprehensive Database of Escherichia Coli Biology. *Nucleic Acids Res.* **2011**, *39*, D583–D590. [[CrossRef](#)]
30. Keseler, I.M.; Gama-Castro, S.; Mackie, A.; Billington, R.; Bonavides-Martinez, C.; Caspi, R.; Kothari, A.; Krummenacker, M.; Midford, P.E.; Muñoz-Rascado, L.; et al. The EcoCyc Database in 2021. *Front. Microbiol.* **2021**, *12*, 711077. [[CrossRef](#)]
31. Christman, M.F.; Morgan, R.W.; Jacobson, F.S.; Ames, B.N. Positive Control of a Regulon for Defenses against Oxidative Stress and Some Heat-Shock Proteins in Salmonella Typhimurium. *Cell* **1985**, *41*, 753–762. [[CrossRef](#)]
32. Seaver, L.C.; Imlay, J.A. Hydrogen Peroxide Fluxes and Compartmentalization inside Growing Escherichia Coli. *J. Bacteriol.* **2001**, *183*, 7182–7189. [[CrossRef](#)]
33. Schellhorn, H.E.; Hassan, H.M. Transcriptional Regulation of KatE in Escherichia Coli K-12. *J. Bacteriol.* **1988**, *170*, 4286–4292. [[CrossRef](#)]
34. Sezonov, G.; Joseleau-Petit, D.; D'Ari, R. Escherichia Coli Physiology in Luria-Bertani Broth. *J. Bacteriol.* **2007**, *189*, 8746–8749. [[CrossRef](#)]
35. Guarino, V.A.; Oldham, W.M.; Loscalzo, J.; Zhang, Y.-Y. Reaction Rate of Pyruvate and Hydrogen Peroxide: Assessing Antioxidant Capacity of Pyruvate under Biological Conditions. *Sci. Rep.* **2019**, *9*, 19568. [[CrossRef](#)]
36. Bond, C.S.; White, M.F.; Hunter, W.N. High Resolution Structure of the Phosphohistidine-Activated Form of Escherichia Coli Cofactor-Dependent Phosphoglycerate Mutase*. *J. Biol. Chem.* **2001**, *276*, 3247–3253. [[CrossRef](#)]
37. Fraser, H.I.; Kvaratskhelia, M.; White, M.F. The Two Analogous Phosphoglycerate Mutases of Escherichia Coli. *FEBS Lett.* **1999**, *455*, 344–348. [[CrossRef](#)]
38. Martinez, A.; Kolter, R. Protection of DNA during Oxidative Stress by the Nonspecific DNA-Binding Protein Dps. *J. Bacteriol.* **1997**, *179*, 5188–5194. [[CrossRef](#)]
39. Sen, A.; Imlay, J.A. How Microbes Defend Themselves From Incoming Hydrogen Peroxide. *Front. Immunol.* **2021**, *12*, 1104. [[CrossRef](#)]

40. Lange, R.; Hengge-Aronis, R. Identification of a Central Regulator of Stationary-Phase Gene Expression in *Escherichia Coli*. *Mol. Microbiol.* **1991**, *5*, 49–59. [[CrossRef](#)]
41. Loewen, P.C.; Triggs, B.L. Genetic Mapping of KatF, a Locus That with KatE Affects the Synthesis of a Second Catalase Species in *Escherichia Coli*. *J. Bacteriol.* **1984**, *160*, 668–675. [[CrossRef](#)]
42. Henard, C.A.; Tapscott, T.; Crawford, M.A.; Husain, M.; Doulias, P.-T.; Porwollik, S.; Liu, L.; McClelland, M.; Ischiropoulos, H.; Vázquez-Torres, A. The 4-Cysteine Zinc-Finger Motif of the RNA Polymerase Regulator DksA Serves as a Thiol Switch for Sensing Oxidative and Nitrosative Stress. *Mol. Microbiol.* **2014**, *91*, 790–804. [[CrossRef](#)]
43. Zhang, A.; Wassarman, K.M.; Ortega, J.; Steven, A.C.; Storz, G. The Sm-like Hfq Protein Increases OxyS RNA Interaction with Target MRNAs. *Mol. Cell* **2002**, *9*, 11–22. [[CrossRef](#)]
44. Muffler, A.; Fischer, D.; Hengge-Aronis, R. The RNA-Binding Protein HF-I, Known as a Host Factor for Phage Qbeta RNA Replication, Is Essential for RpoS Translation in *Escherichia Coli*. *Genes Dev.* **1996**, *10*, 1143–1151. [[CrossRef](#)]
45. Liu, Y.; Imlay, J.A. Cell Death from Antibiotics without the Involvement of Reactive Oxygen Species. *Science* **2013**, *339*, 1210–1213. [[CrossRef](#)]
46. Imlay, J.A.; Linn, S. Mutagenesis and Stress Responses Induced in *Escherichia Coli* by Hydrogen Peroxide. *J. Bacteriol.* **1987**, *169*, 2967–2976. [[CrossRef](#)]
47. Demple, B.; Halbrook, J.; Linn, S. *Escherichia Coli* Xth Mutants Are Hypersensitive to Hydrogen Peroxide. *J. Bacteriol.* **1983**, *153*, 1079–1082. [[CrossRef](#)]
48. Sermon, J.; Wevers, E.M.-R.P.; Jansen, L.; De Spiegeleer, P.; Vanoirbeek, K.; Aertsen, A.; Michiels, C.W. CorA Affects Tolerance of *Escherichia Coli* and *Salmonella Enterica* Serovar Typhimurium to the Lactoperoxidase Enzyme System but Not to Other Forms of Oxidative Stress. *Appl. Environ. Microbiol.* **2005**, *71*, 6515–6523. [[CrossRef](#)]
49. Shimada, T.; Kori, A.; Ishihama, A. Involvement of the Ribose Operon Repressor RbsR in Regulation of Purine Nucleotide Synthesis in *Escherichia Coli*. *FEMS Microbiol. Lett.* **2013**, *344*, 159–165. [[CrossRef](#)]
50. Wan, Y.; Wang, M.; Chan, E.W.C.; Chen, S. Membrane Transporters of the Major Facilitator Superfamily Are Essential for Long-Term Maintenance of Phenotypic Tolerance to Multiple Antibiotics in *E. Coli*. *Microbiol. Spectr.* **2021**, *9*, e0184621. [[CrossRef](#)]
51. Rungrasamee, W.; Liu, X.; Pomposiello, P.J. Activation of Glucose Transport under Oxidative Stress in *Escherichia Coli*. *Arch. Microbiol.* **2008**, *190*, 41–49. [[CrossRef](#)]
52. Varghese, S.; Tang, Y.; Imlay, J.A. Contrasting Sensitivities of *Escherichia Coli* Aconitases A and B to Oxidation and Iron Depletion. *J. Bacteriol.* **2003**, *185*, 221–230. [[CrossRef](#)]
53. Park, S.J.; Gunsalus, R.P. Oxygen, Iron, Carbon, and Superoxide Control of the Fumarase FumA and FumC Genes of *Escherichia Coli*: Role of the ArcA, Fnr, and SoxR Gene Products. *J. Bacteriol.* **1995**, *177*, 6255–6262. [[CrossRef](#)]
54. Jozefczuk, S.; Klie, S.; Catchpole, G.; Szymanski, J.; Cuadros-Inostroza, A.; Steinhauser, D.; Selbig, J.; Willmitzer, L. Metabolomic and Transcriptomic Stress Response of *Escherichia Coli*. *Mol. Syst. Biol.* **2010**, *6*, 364. [[CrossRef](#)]
55. Radin, J.N.; Kelliher, J.L.; Solórzano, P.K.P.; Grim, K.P.; Ramezanifard, R.; Schlauch, J.M.; Kehl-Fie, T.E. Metal-Independent Variants of Phosphoglycerate Mutase Promote Resistance to Nutritional Immunity and Retention of Glycolysis during Infection. *PLoS Pathog.* **2019**, *15*, e1007971. [[CrossRef](#)]
56. Foster, J.M.; Davis, P.J.; Raverdy, S.; Sibley, M.H.; Raleigh, E.A.; Kumar, S.; Carlow, C.K.S. Evolution of Bacterial Phosphoglycerate Mutases: Non-Homologous Isofunctional Enzymes Undergoing Gene Losses, Gains and Lateral Transfers. *PLoS ONE* **2010**, *5*, e13576. [[CrossRef](#)]
57. Imlay, J.A. The Molecular Mechanisms and Physiological Consequences of Oxidative Stress: Lessons from a Model Bacterium. *Nat. Rev. Microbiol.* **2013**, *11*, 443–454. [[CrossRef](#)]